



# Model-based Predictive and Backstepping controllers for a state coupled four-tank system with bounded control inputs: A comparative study

Houssemmedine Gouta<sup>\*</sup>, Salim Hadj Said<sup>1</sup>, Faouzi M'sahli<sup>2</sup>

*Research Unit of Industrial Systems Study and Renewable Energy (ESIER), National Engineering School of Monastir (ENIM), University of Monastir, Ibn El Jazzar, 5019 Monastir, Tunisia*

Received 14 March 2015; received in revised form 26 June 2015; accepted 10 August 2015

## Abstract

This paper investigates the problem of global tracking control design for a state coupled four-tank liquid level system with bounded control inputs. For this MIMO system's dynamics, motivated by a desire to provide precise liquid level control, two radically different control approaches are presented and compared: the nonlinear generalized predictive control (NGPC) and the Backstepping control. First, an analytical solution of the NGPC is developed based on the nominal model. Then, a nonlinear Backstepping controller is designed in order to ensure globally asymptotical stabilization for this nonlinear system. To ensure a suitable basis for their comparison, the two different control methods are designed and verified with the same test setup under the control input saturation imposed by the system's actuators. To highlight the efficiency and applicability of the proposed control schemes, simulation as well as experimental results are provided and discussed.

© 2015 The Franklin Institute. Published by Elsevier Ltd. All rights reserved.

**Keywords:** Backstepping control; Predictive control; Inputs saturation; Stability; Experimental validation; Comparative study

<sup>\*</sup>Corresponding author. Tel.: +216 97 117 564.

E-mail addresses: [gouta.houssem@gmail.com](mailto:gouta.houssem@gmail.com) (H. Gouta), [salim.hadjsaid@issig.rnu.tn](mailto:salim.hadjsaid@issig.rnu.tn) (S. Hadj Said), [faouzi.msahli@enim.rnu.tn](mailto:faouzi.msahli@enim.rnu.tn) (F. M'sahli).

<sup>1</sup>Tel.: +216 94 458 002.

<sup>2</sup>Tel.: +216 98 229 126.

<http://dx.doi.org/10.1016/j.jfranklin.2015.08.004>

0016-0032/© 2015 The Franklin Institute. Published by Elsevier Ltd. All rights reserved.

## 1. Introduction

Liquid level control is needed in various industrial applications, e.g., in food processing, water purification systems, filtration, pharmaceutical industries, decoration, boilers, dairy, beverage, nuclear power generation plants, industrial chemical processing, spray coating, automatic liquid dispensing and replenishment devices. For the purpose of feedback control, typical actuators are widely used such as electrical pumps and motorized valves, and many types of level sensors provide liquid level measurement such as displacement float, pressure sensors, etc. [1].

This paper introduces the control of a state coupled four-tank system (Fig. 1). This plant is inspired from the studied hybrid liquid level system in [24] and it represents a modified version of the quadruple-tank process presented in [2] which has proven to be a very interesting system for control education and for the validation of advanced multivariable control techniques [16,26]. Since this system is highly coupled, this can exhibit transmission zero dynamics, its dynamics are nonlinear and the states and inputs are subjected to hard constraints. Furthermore, the studied four-tank plant is implemented using industrial instrumentation and is safe to use. The quadruple-tank process has been used to illustrate various control strategies including internal model control [3], dynamic matrix control [4], multivariable robust control [5] and distributed model Predictive control [6,26].

Among the numerous existing approaches of nonlinear approaches in industrial control, the MPC approach [10] and the Backstepping approach [11] are selected. The reason for this choice is the radical difference between them. In fact, Backstepping is a theoretical strategy, yielding to an explicit stabilizing control law. On the contrary, MPC is an efficient practical strategy which suffers from the lack of theoretical stability result in certain cases due to the implicit numerical control law. Moreover, the Backstepping approach is chosen because it is the recently control used for an analogous SISO liquid level system and it gives better performances than the proportional plus integral controller control method [23,27]. This method is chosen to compare its performances with the NGPC approach which presents the time continuous solution of nonlinear MPC approach and which is recently applied to complex systems such as small-scale helicopter [34], induction motor [13], etc. Additionally, both these approaches of control can be applied to the class of input affine nonlinear systems to which the studied process belongs.

To achieve a good tracking performance, this paper firstly adopts a nonlinear generalized predictive control (NGPC) strategy. It is known that the model predictive control strategy uses a model to predict the future behavior of the studied plant, and then an optimal control decision can be made based on

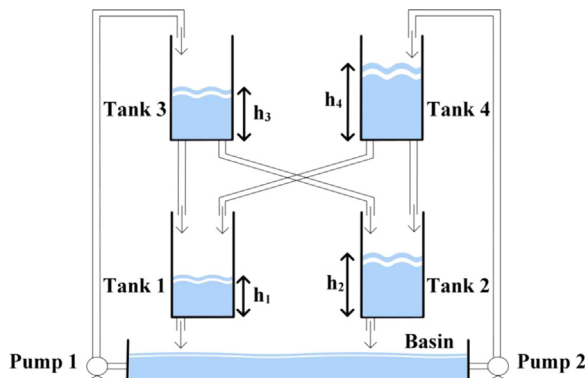


Fig. 1. State coupled four-tank system.

optimization according to the prediction [12]. This “foresee” feature of MPC makes it a suitable control strategy for autonomous liquid level systems. Especially for the trajectory tracking problem, the MPC can take into account the future value of the reference to improve the performance in the sense that not only the current tracking error can be suppressed but also the future errors.

The MPC technique generally requires the solution of an optimization problem (OP) at every sampling instant. This poses an obstacle on the real-time implementation due to the heavy computational burden. In this paper, the proposed algorithm tackles the nonlinear dynamics of a state coupled four-tank system. An analytical solution to the nonlinear MPC can be found by approximating the tracking error and control efforts in a receding horizon using their Taylor expansion to a specified order, and consequently the closed form controller can be formulated without online optimization [13–15].

On the other hand, this paper adopts also the Backstepping approach. This control strategy was initially developed to provide a generic procedure for synthesizing Lyapunov stabilizing control laws for triangular nonlinear ordinary differential equations (ODEs) systems by Kanellakopoulos et al. [18]. Therewith, extensions to the control of linear partial derivative equations (PDEs) were recently reported by Krstic and Smyshlyaev [11] and extensions to the control of a nonlinear SISO liquid level system (see [23] and [27]). Moreover, Backstepping technique is used in some adaptive neural methods to study the control problems of uncertain nonlinear systems [29–31] as well as in several globally stable approximation-based adaptive neural control schemes developed for the uncertain systems free of time delays [32].

However, the effect of saturation nonlinearity has not been addressed with these previous approaches although saturation, dead zone, backlash, and hysteresis are the most common non-smooth actuator nonlinearities in practical control systems that arise from physical and technological constraints. Their presence severely degrades the control system performance [7–9] and gives rise to undesirable inaccuracy or leads to instability [35], especially for the two studied approaches in this paper. So inputs saturation has to be considered when the controller is designed in practical industrial process control field.

To solve such a problem, certain modifications of standard Backstepping controllers are required. A preliminary result for a class of single input uncertain nonlinear systems in the presence of input saturation and external disturbance is reported in [8]. Recently, an adaptive neural Backstepping controller is proposed for a class of strict-feedback nonlinear systems with unknown input saturation using a smooth non-affine function of the control input signal to approximate the input saturation function [36]. Furthermore, another adaptive neural Backstepping control scheme is proposed for a class of strict-feedback nonlinear systems with unmodelled dynamics, dynamic disturbances and input saturation [17].

Additionally, the influence that bounded control inputs to the MPC approach is treated by applying a method dealing with input constraints which is the use of saturated control [37–39]. Using this method, the proposed MPC design algorithms permit the controller to saturate. Hence, it can lead to the reduction of the conservativeness. Using the method mentioned in [39], the most recent predictive method presents a sampled-data MPC design for continuous-time linear parameter varying (LPV) systems with input constraints [40].

Different publications and approaches such as those presented in the previous paragraphs for every proposed control method as well as some comparative studies of these control approaches on other processes [19] and with other approaches [20] can be found in the literature, but until now (as far as the authors know), no comparative study between these control approaches in application on liquid level systems has been presented in the literature. This paper utilizes nonlinear Backstepping technique and NGPC approach on the nonlinear dynamics of a

state-coupled, four-tank, liquid level system to develop controllers with trajectory tracking capabilities in the presence of inputs saturation. A model-based nonlinear Predictive controller and a Backstepping controller are designed. Moreover, this paper presents a survey and a detailed experimental comparative study to facilitate the choice of control approach for controlling such a liquid level system. Based on the given didactic system with available sensor system and achievable computation power for the control implementation, this paper determines which of the considered control approaches the optimal choice in terms of dynamic behavior is. Indeed, the theoretical and practical analysis will highlight that the choice of the optimal control approach is dependent on the complexity of the applied control structure and the desired control performance. To ensure a suitable basis for their comparison, the two different control methods are designed and verified with the same test setup.

This paper is structured as follows. In Section 2, the state coupled four-tank system description and its mathematical model will be introduced. The liquid level NGPC approach that is to be considered is presented in Section 3. Section 4 introduces a study of the global stability of the used Backstepping technique for a particular class of MIMO systems as well as the design of the Backstepping controller for the quadruple tank process. In Section 5, simulation and experimental results are presented to demonstrate the efficiency and the applicability of the proposed approaches as well as a detailed comparison of the measurement results. Finally, some concluding remarks are given in Section 6.

## 2. System model and problem formulation

### 2.1. Process modeling

The schematic drawing in Fig. 1 presents the model of a two degree-of-freedom (DOF) state coupled four-tank system. This system consists of a liquid basin, two pumps, four tanks having same area with orifices and level sensors at the bottom of each tank. In this experimental setup, Pump 1 and Pump 2 provide respectively in feed to Tank 3 and Tank 4 and the outflows of Tank 3 and Tank 4 become in feed to Tank 1 and Tank 2 as shown in Fig. 1. The outflow of Tank 1 and Tank 2 are emptied into the liquid basin. With regard to the system dynamic model, the following assumptions are used to describe the level of liquid in the four tanks:

- i. The liquid levels  $h_1$ ,  $h_2$ ,  $h_3$  and  $h_4$  are measured by four pressure sensors.
- ii. The liquid levels in the four tanks are always greater than 3 cm and less than 30 cm.
- iii.  $Y = [h_1 \ h_2]^T$  presents the output of the system.
- iv.  $U_a = [u_{a1} \ u_{a2}]^T$ , where  $u_{a1}$  and  $u_{a2}$  which are the voltages applied respectively at the input terminals of Pump 1 and Pump 2 (Both are bounded by 0 and 12 V), represent the inputs of the system.

Based on the above assumptions, the dynamic equations for the liquid level in the four tanks are derived as follows. The time rate of change of liquid level in each tank is given by

$$\dot{h}_i(t) = \frac{1}{S_i} (F_i^{in}(t) - F_i^{out}(t)), \quad i = 1, 2, 3, 4 \quad (1)$$

where  $h_i(t)$ ,  $S_i$ ,  $F_i^{in}(t)$  and  $F_i^{out}(t)$  are the liquid level, cross-sectional area, inflow rate, and outflow rate, respectively, for the  $i$ th tank. Given that both pumps are identical, the inflow rates

into the two top tanks 3 and 4 are given by

$$\begin{cases} F_3^{in}(t) = K_p u_{a1}(t) \\ F_4^{in}(t) = K_p u_{a2}(t) \end{cases} \quad (2)$$

where  $K_p$  is the pumps constant ( $\text{cm}^3/\text{V}$ ). Such that, using Bernoulli's law for the flow through small orifices [21], the outflow velocity from the orifice at the bottom of each tank is

$$V_i^{out}(t) = \sqrt{2gh_i(t)}, \quad i = 1, 2, 3, 4 \quad (3)$$

then, the outflow rate for each top tank is given by

$$F_i^{out}(t) = (s_{i1} + s_{i2})\sqrt{2gh_i(t)}, \quad i = 3, 4 \quad (4)$$

where  $g$  is the gravitational acceleration and  $s_{ij}$  denotes the cross-sectional areas of the outflow orifice at the bottom of the  $i$ th tank into the  $j$ th tank, and for each bottom tank

$$F_i^{out}(t) = s_i\sqrt{2gh_i(t)}, \quad i = 1, 2 \quad (5)$$

where  $s_i$  denotes the cross-sectional area of the outflow orifice at the bottom of the  $i$ th tank into the basin ( $i = 1, 2$ ). Finally, note that for the four-tank liquid level system

$$F_1^{in}(t) + F_2^{in}(t) = F_3^{out}(t) + F_4^{out}(t) \quad (6)$$

Thus, the following dynamic equation for the system is obtained:

$$\begin{cases} \dot{h}_1(t) = -\frac{s_1}{S_1}\sqrt{2gh_1(t)} + \frac{s_{31}}{S_3}\sqrt{2gh_3(t)} + \frac{s_{41}}{S_4}\sqrt{2gh_4(t)} \\ \dot{h}_2(t) = -\frac{s_2}{S_2}\sqrt{2gh_2(t)} + \frac{s_{32}}{S_3}\sqrt{2gh_3(t)} + \frac{s_{42}}{S_4}\sqrt{2gh_4(t)} \\ \dot{h}_3(t) = -\frac{s_{31}+s_{32}}{S_3}\sqrt{2gh_3(t)} + \frac{K_p}{S_3}u_{a1}(t) \\ \dot{h}_4(t) = -\frac{s_{41}+s_{42}}{S_4}\sqrt{2gh_4(t)} + \frac{K_p}{S_4}u_{a2}(t) \end{cases} \quad (7)$$

In this case, Eq. (7) can be written as the following system:

$$\begin{cases} \dot{h}_1(t) = -c_1\sqrt{h_1(t)} + c_2\sqrt{h_3(t)} + c_3\sqrt{h_4(t)} \\ \dot{h}_2(t) = -c_4\sqrt{h_2(t)} + c_5\sqrt{h_3(t)} + c_6\sqrt{h_4(t)} \\ \dot{h}_3(t) = -c_7\sqrt{h_3(t)} + c_8u_{a1}(t) \\ \dot{h}_4(t) = -c_9\sqrt{h_4(t)} + c_{10}u_{a2}(t) \end{cases} \quad (8)$$

Consider that the four tanks have the same cross-sectional area ( $S_i = S_j$ ,  $i \neq j$ ) as well as  $s_{32} = s_{41}$  and  $s_{31} = s_{42}$ . In addition, Tanks 1 and 2 have the same orifice diameter ( $s_1 = s_2$ ). Consequently, for our quadruple tank process we have:  $c_1 = c_4$ ,  $c_2 = c_6$ ,  $c_3 = c_5$ ,  $c_7 = c_9$  and  $c_8 = c_{10}$ .

## 2.2. Actuators saturation

In control engineering, the most commonly used actuators are continuous drive devices, along with some incremental drive actuators such as DC motors to which belong the pumps of our system. Saturation linearity with its maximum and minimum operation limits is unavoidable in such devices. As shown in Fig. 2,  $U_a$  and  $U$  present respectively the actuators input voltage and the control inputs. Taking into account the fourth assumption of the dynamic model, this paper studies actuator saturation that appears in the considered state coupled four-tank system and

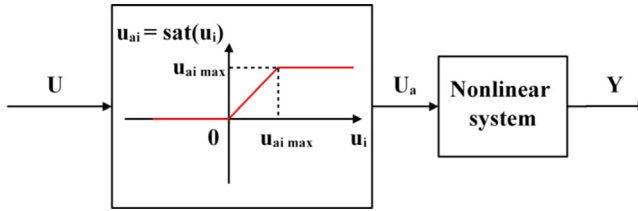


Fig. 2. Nonlinear plant with actuators saturation.

evaluates the comportment of two nonlinear controllers under this operating condition. Fig. 2 shows the linear saturation  $u_{ai} = \text{sat}(u_i)$ , where  $u_{ai}$  and  $u_i$  are scalars,  $i = 1, 2$ . Saturation limits are given by 0 and  $u_{ai \max}$ .

Mathematically, the input voltages of the two actuators (pumps) of the plant  $u_{a1}$  and  $u_{a2}$  are given by

$$u_{ai} = \begin{cases} u_{ai \max} & \text{if } u_i \geq u_{ai \max} \\ u_i(t) & \text{if } 0 \leq u_i \leq u_{ai \max}, \quad i = 1, 2 \\ 0 & \text{if } u_i \leq 0 \end{cases} \quad (9)$$

where  $u_{ai \max} = 12V$  is the maximal input voltage for the two pumps. If the control signal  $u_i(t)$  falls outside the range of the actuators, input saturation occurs and the control input  $u_{ai}(t)$  cannot be fully implemented by the device.

In the next sections, we assume that the four sensors are available to measure the liquid levels in the four tanks. Taking into account the inputs saturation, two control schemes are designed and applied to control the liquid levels  $h_1$  and  $h_2$  with respect to two desired references respectively  $r_1$  and  $r_2$ .

### 3. Output feedback Predictive controller design

#### 3.1. Nonlinear generalized predictive control (NGPC)

In the spirit of the state NGPC design given in [14], an output feedback controller is developed that can be efficiently applied to the state coupled four-tank system. To synthesize the state feedback controller, we consider the following assumptions:

**Assumption 1.** There exists a globally Lipschitz diffeomorphism  $\phi : \mathcal{R}^4 \rightarrow \mathcal{R}^4$  that transforms the system (8) into the following form described by

$$\begin{cases} \dot{Z} = IZ + J(b(Z)U + g(Z)) + \psi(Z) \\ Y = LZ \end{cases} \quad (10)$$

where  $I = \begin{bmatrix} 0_2 & I_2 \\ 0_2 & 0_2 \end{bmatrix}$ ,  $J = \begin{bmatrix} 0_2 \\ I_2 \end{bmatrix}$ ,  $L = [I_2 \quad 0_2]$ ,  $b(Z) \in \mathcal{R}^{2 \times 2}$ ,  $g(Z) \in \mathcal{R}^2$  and

$\psi(Z) = \begin{bmatrix} \psi_1(Z_1) \\ \psi_2(Z_1, Z_2) \end{bmatrix} \in \mathcal{R}^4$ , with  $Z = [Z_1^T \quad Z_2^T]^T = [z_1 \quad z_2 \quad z_3 \quad z_4]^T$  is the internal state

of the system ( $Z \in \mathcal{Z} \subset \mathcal{R}^4$ ),  $U \in \mathcal{U} \subset \mathcal{R}^2$  the control input,  $Y \in \mathcal{R}^2$  the measured output,

$$I_2 = \begin{bmatrix} 1 & 0 \\ 0 & 1 \end{bmatrix} \text{ and } 0_2 = \begin{bmatrix} 0 & 0 \\ 0 & 0 \end{bmatrix}.$$

**Assumption 2.** The nonlinear functions  $\psi(\cdot)$ ,  $b(\cdot)$  and  $g(\cdot)$  are globally Lipschitz in  $Z$ .

**Assumption 3.** The output  $Y(t)$  and the reference signal  $R(t)$  are sufficiently many times continuously differentiable with respect to  $t$ .

An optimal tracking problem can be stated as follows: design a controller such that the closed-loop system is asymptotically stable and the output  $Y(t)$  of the nonlinear system (10) optimally tracks the prescribed reference  $R(t)$  in terms of a given performance index.

Taking into account the structure of system (10), it is possible to derive the subsystem desired state trajectory  $Z_d(t) = [Z_{1d}^T \ Z_{2d}^T]^T \in \mathcal{R}^4$  and the associated input  $U_d(t)$  corresponding to the desired trajectory  $R = Z_{1d}$ . This allows defining an admissible reference model as follows:

$$\dot{Z}_d = IZ_d + J(b(Z_d)U_d + g(Z_d)) + \psi(Z_d) \quad (11)$$

According to Eq. (10), the state reference trajectory  $Z_{2d}$  and the desired control  $U_d$  are extracted as follows:

$$\begin{cases} Z_{2d} = \dot{Z}_{1d} - \psi_1(Z_{1d}) \\ U_d = b(Z_d)^{-1}(\dot{Z}_{2d} - g(Z_d) - \psi_2(Z_{1d}, Z_{2d})) \end{cases} \quad (12)$$

The basic idea of the moving-horizon control is, at any time  $t$ , to design within a moving time frame located at time  $t$  regarding  $Z(t)$  as the initial condition of a state trajectory  $\hat{Z}(t + \tau)$  with associated predicted  $\hat{Y}(t + \tau)$ . To distinguish them from the real variables, the hatted variables are defined as the variables in the moving time frame. In the NGPC strategy, tracking control can be achieved by minimizing the moving-horizon performance index  $\mathcal{J} \in \mathcal{R}$  which is given by

$$\mathcal{J} = \frac{1}{2} \int_0^{T_p} (\hat{Y}(t + \tau) - \hat{R}(t + \tau))^T (\hat{Y}(t + \tau) - \hat{R}(t + \tau)) d\tau \quad (13)$$

where  $T_p$  is the predictive period,  $\hat{R} = [\hat{r}_1 \ \hat{r}_2]^T$  is the prescribed tracking reference [28].

According to Assumption 3, the outputs  $\hat{Y}(t + \tau)$  and  $\hat{R}(t + \tau)$  at the time  $\tau$  are approximately predicted by their Taylor-series expansion up to order 2 as follows:

$$\hat{Y}(t + \tau) \doteq \bar{\mathcal{T}}(\tau) \bar{Y}(t) \quad (14)$$

$$\hat{R}(t + \tau) \doteq \bar{\mathcal{T}}(\tau) \bar{R}(t) \quad (15)$$

where  $\bar{\mathcal{T}}(\tau) = [I_2 \ \tau I_2 \ \frac{\tau^2}{2!} I_2]$ ,  $\bar{Y}(t) = [Y^T(t) \ \dot{Y}^T(t) \ \ddot{Y}^T(t)]^T$  and

$$\bar{R}(t) = [R^T(t) \ \dot{R}^T(t) \ \ddot{R}^T(t)]^T.$$

Hence,  $\mathcal{J}$  can be written in matrix form as follows:

$$\mathcal{J} = \frac{1}{2} (\bar{Y}(t) - \bar{R}(t))^T \mathcal{T}(T_p) (\bar{Y}(t) - \bar{R}(t)) \quad (16)$$



where

$$\mathcal{T}(T_p) = \int_0^{T_p} \overline{\mathcal{T}}^T(\tau) \overline{\mathcal{T}}(\tau) d\tau \quad (17)$$

The  $ij$ th elements of the square matrix  $\mathcal{T}(T_p)$  are in the form  $\mathcal{T}_{(ij)} = \frac{T_p^{i+j-1}}{(i+j-1)(i-1)!(j-1)!} I_2$  with  $i, j = 1, 2, 3$ .

The differentiation of the output  $Y(t)$  with respect to  $t$  gives

$$\begin{cases} Y = Z_1 \\ \dot{Y} = Z_2 + \psi_1(Z_1) \\ \ddot{Y} = b(Z)U + g(Z) + \dot{\psi}_1(Z_1) + \psi_2(Z_1, Z_2) \end{cases} \quad (18)$$

In addition, the differentiation of the benchmark  $R(t)$  with respect to  $t$  gives

$$\begin{cases} R = Z_{1d} \\ \dot{R} = Z_{2d} + \psi_1(Z_{1d}) \\ \ddot{R} = b(Z_d)U_d + g(Z_d) + \dot{\psi}_1(Z_{1d}) + \psi_2(Z_{1d}, Z_{2d}) \end{cases} \quad (19)$$

Let

$$\overline{Y}(t) - \overline{R}(t) = M(Z, Z_d) + \begin{bmatrix} 0_{2 \times 1} \\ 0_{2 \times 1} \\ N(Z, U) \end{bmatrix} \quad (20)$$

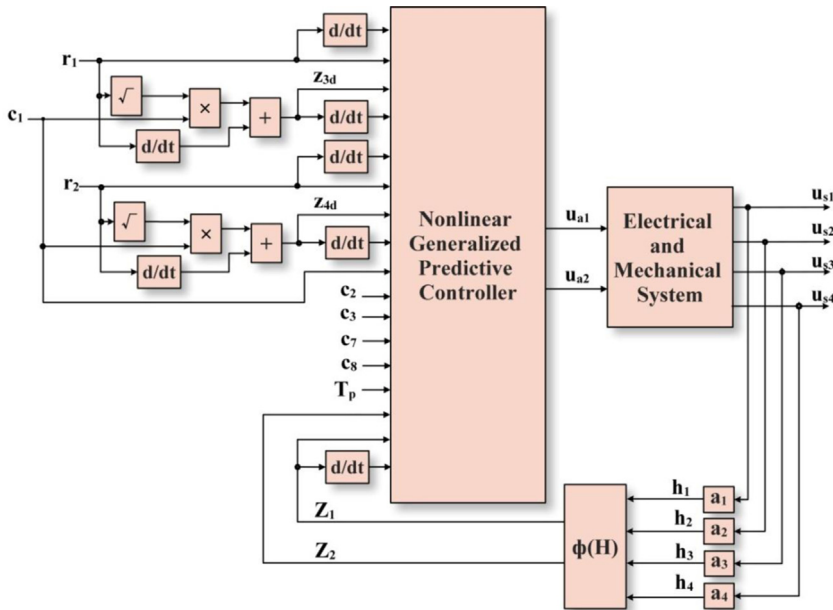


Fig. 3. Block diagram of the NGPC approach.



$$\text{where } M(Z, Z_d) = \begin{bmatrix} e_{1Z} \\ e_{2Z} + \Delta\psi_1 \\ -b(Z_d)U_d + \Delta g + d\psi_1 + \Delta\psi_2 \end{bmatrix}, N(Z, U) = b(Z)U, 0_{2 \times 1} = \begin{bmatrix} 0 \\ 0 \end{bmatrix},$$

$$e_{1Z} = \begin{bmatrix} z_1 - r_1 \\ z_2 - r_2 \end{bmatrix}, e_{2Z} = \begin{bmatrix} z_3 - z_{3d} \\ z_4 - z_{4d} \end{bmatrix}, \Delta\psi_1 = \psi_1(Z_1) - \psi_1(R), \Delta g = g(Z_1) - g(R),$$

$$d\psi_1 = \dot{\psi}_1(Z_1) - \dot{\psi}_1(R) \text{ and } \Delta\psi_2 = \psi_2(Z_1, Z_2) - \psi_2(R, Z_{2d}).$$

A simple computation implies that (16) can be written as follows:

$$\mathcal{J} = \frac{1}{2} (M^T \mathcal{T} (T_p) M + 2M^T \overline{\mathcal{T}}_{c3} N + \mathcal{T}_{\{3,3\}} N^T N) \quad (21)$$

where  $\mathcal{T}_{c3} = \begin{bmatrix} \frac{T^3}{6} I_2 & \frac{T^4}{8} I_2 & \frac{T^5}{20} I_2 \end{bmatrix}^T$  is the sub-matrix composed of the 5th and 6th columns and

$\mathcal{T}_{\{3,3\}} = \frac{T^5}{20} I_2$  is the (3, 3)th sub-matrix of matrix  $\mathcal{T}(T_p)$ .

An analytic solution of predictive control arises from the derivative of the cost function  $\mathcal{J}$  with respect to the control input  $U$ , and it is given by

$$\frac{\partial \mathcal{J}}{\partial U} = \frac{1}{2} (2M^T \overline{\mathcal{T}}_{c3} b(Z) + 2U^T b(Z)^T b(Z) \mathcal{T}_{\{3,3\}}) = \begin{bmatrix} 0 & 0 \end{bmatrix} = 0_{1 \times 2} \quad (22)$$

So we have

$$U = \begin{bmatrix} u_1 \\ u_2 \end{bmatrix} = b(Z)^{-1} \left( -\mathcal{T}_{\{3,3\}}^{-1} \overline{\mathcal{T}}_{c3}^T M \right) \quad (23)$$

By replacing  $U_d$  in (23) by its expression given in (12), the NGPC law can be given by the following expression:

$$U = b(Z)^{-1} (\dot{Z}_{2d} - g(Z) + \gamma(e_Z)) \quad (24)$$

where  $\gamma(e_Z) = -(K_1 e_{1Z} + K_2 (e_{2Z} + \Delta\psi_1) + d\psi_1 + \psi_2(Z_1, Z_2))$ ,  $K_1 = \mathcal{T}_{\{3,3\}}^{-1} \mathcal{T}_{\{3,1\}}$  and  $K_2 = \mathcal{T}_{\{3,3\}}^{-1} \mathcal{T}_{\{3,2\}}$ .

### 3.2. NGPC liquid level controller design

The proposed NGPC method, whose block diagram is shown in Fig. 3, is applied to control the liquid levels  $h_1$  and  $h_2$  with respect to the desired benchmark  $R = [r_1 \ r_2]^T$  such as  $3 \leq r_i \leq 30$  cm  $i = 1, 2$ . To synthesize the state feedback controller, model (8) shall be transformed to new coordinates for which the design is easier. By applying the diffeomorphism  $\phi$  which is globally Lipschitz ( $h_i > 1$ ,  $i = 3, 4$ ) according to Eq. (23)

$$Z = \phi(H) = \begin{bmatrix} z_1 \\ z_2 \\ z_3 \\ z_4 \end{bmatrix} = \begin{bmatrix} h_1 \\ h_2 \\ c_2 \sqrt{h_3} + c_3 \sqrt{h_4} \\ c_5 \sqrt{h_3} + c_6 \sqrt{h_4} \end{bmatrix} \quad (25)$$

we obtain the system in the new coordinates as

$$\begin{cases} \dot{z}_1 = -c_1\sqrt{z_1} + z_3 \\ \dot{z}_2 = -c_4\sqrt{z_2} + z_4 \\ \dot{z}_3 = -\alpha_3 + \alpha\left(\frac{c_2c_8}{\alpha_1}u_1 + \frac{c_3c_{10}}{\alpha_2}u_2\right) \\ \dot{z}_4 = -\alpha_4 + \alpha\left(\frac{c_5c_8}{\alpha_1}u_1 + \frac{c_6c_{10}}{\alpha_2}u_2\right) \end{cases} \quad (26)$$

where  $\alpha = \frac{1}{2}(c_2c_6 - c_3c_5)$ ,  $\alpha_1 = c_6z_3 - c_3z_4$ ,  $\alpha_2 = -c_5z_3 + c_2z_4$ ,  $\alpha_3 = \frac{1}{2}(c_2c_7 + c_3c_9)$  and  $\alpha_4 = \frac{1}{2}(c_5c_7 + c_6c_9)$ .

This can be written in the form (10) as

$$\begin{cases} \dot{Z} = \begin{bmatrix} \dot{z}_1 \\ \dot{z}_2 \end{bmatrix} = IZ + J(b(Z)U + g(Z)) + \psi(Z) \\ Y = LZ = Z_1 \end{cases} \quad (27)$$

where  $b(Z) = \alpha \begin{bmatrix} \frac{c_2c_8}{\alpha_1} & \frac{c_3c_{10}}{\alpha_2} \\ \frac{c_5c_8}{\alpha_1} & \frac{c_6c_{10}}{\alpha_2} \end{bmatrix}$ ,  $g(Z) = \begin{bmatrix} -\alpha_3 \\ -\alpha_4 \end{bmatrix}$ ,  $I = \begin{bmatrix} 0_2 & I_2 \\ 0_2 & 0_2 \end{bmatrix}$ ,  $J = \begin{bmatrix} 0_2 \\ I_2 \end{bmatrix}$ ,  $L = [I_2 \quad 0_2]$  and

$$\psi(Z) = \begin{bmatrix} -c_1\sqrt{z_1} \\ -c_4\sqrt{z_2} \\ 0 \\ 0 \end{bmatrix}.$$

An explicit control law can be derived from Eq. (24) as the following ( $\psi_2(Z_1, Z_2) = 0_{2 \times 1}$ ):

$$U = b(Z)^{-1}(\dot{Z}_{2d} - g(Z) - K_1e_{1Z} - K_2(e_{2Z} + \Delta\psi_1) - d\psi_1) \quad (28)$$

where  $b(Z)^{-1} = \text{inv}(b(Z))$ ,  $\dot{Z}_{2d} = \begin{bmatrix} \ddot{r}_1 + \frac{c_1\dot{r}_1}{2\sqrt{r_1}} \\ \ddot{r}_2 + \frac{c_4\dot{r}_2}{2\sqrt{r_2}} \end{bmatrix}$ ,  $\Delta\psi_1 = \begin{bmatrix} -c_1(\sqrt{z_1} - \sqrt{r_1}) \\ -c_4(\sqrt{z_2} - \sqrt{r_2}) \end{bmatrix}$ ,  $d\psi_1 = \begin{bmatrix} \frac{-c_1}{2}\left(\frac{\dot{z}_1}{\sqrt{z_1}} - \frac{\dot{r}_1}{\sqrt{r_1}}\right) \\ \frac{-c_4}{2}\left(\frac{\dot{z}_2}{\sqrt{z_2}} - \frac{\dot{r}_2}{\sqrt{r_2}}\right) \end{bmatrix}$ ,

$$K_1 = \frac{10}{3T_p^2}I_2 \text{ and } K_2 = \frac{5}{2T_p}I_2.$$

## 4. Output feedback Backstepping controller design

### 4.1. Stability analysis of the controller design

To study the stability of the Backstepping control, consider the following class of second order nonlinear systems:

$$\begin{cases} \dot{X}_1 = \varphi(X_1) + X_2 \\ \dot{X}_2 = V \\ Y = X_1 \end{cases} \quad (29)$$

where  $Y \in \mathfrak{R}^2$ ,  $V \in \mathfrak{R}^2$ ,  $[X_1^T \quad X_2^T]^T = [x_1 \quad x_2 \quad x_3 \quad x_4]^T \in \mathfrak{R}^4$  and  $\varphi(X_1) = \begin{bmatrix} \varphi_1(x_1) \\ \varphi_2(x_2) \end{bmatrix}$  is

the nonlinear Lipschitz function of the system (29) which is on strict-feedback form [33] and has relative degree two. To begin, let the control objective be to achieve global asymptotic stabilization around a benchmark trajectory  $R \in \mathfrak{R}^2$ .

The proposed Backstepping law is given by the following theorem:

**Theorem 1.** Consider the MIMO system given by Eq. (29), let  $R = [r_1 \ r_2]^T \in \mathfrak{R}^2$  be a benchmark signal with bounded time derivative and let the four assumptions hold:

- A1 :  $\varphi_i(0) = 0$  and  $\max_{x_i \neq r_i} \frac{\varphi_i(x_i) - \varphi_i(r_i)}{x_i - r_i} < \infty \quad \forall \ r_i \in \mathfrak{R}^+$
- A2 :  $(\Delta\varphi_1 - \Delta\vartheta_1 - \dot{r}_1)(x_1 - r_1) + (\Delta\varphi_2 - \Delta\vartheta_2 - \dot{r}_2)(x_2 - r_2) < 0, \quad x_i \neq r_i$
- A3 :  $[\vartheta'(X_1)(\Delta\varphi - \Delta\vartheta - \dot{R}) + (\vartheta'_R(X_1) + \varphi'(R) - \vartheta'(R))\dot{R}]^T (\Delta\varphi - \Delta\vartheta - \dot{R}) > 0$

where  $\Delta\varphi = \varphi(X_1) - \varphi(R) = \begin{bmatrix} \Delta\varphi_1 \\ \Delta\varphi_2 \end{bmatrix}$ ,  $\Delta\vartheta = \vartheta(X_1) - \vartheta(R) = \begin{bmatrix} \Delta\vartheta_1 \\ \Delta\vartheta_2 \end{bmatrix}$  and  $i = 1, 2$ .  
Then the control law is

$$V = -(kI_2 + \vartheta'(X_1))(\varphi(R) + X_2 + \vartheta(X_1) - \vartheta(R)) \quad (30)$$

where  $k \in \mathfrak{R}^+$  and  $\vartheta : \mathfrak{R}^2 \rightarrow \mathfrak{R}^2$  makes  $Y = R$  a globally asymptotically stable equilibrium.

**Proof.** The proof is inspired from the development given in Krstic's works [22] and is an extension of Gouta's works in [23].

Consider the system (29) and let the following change of variable:

$$\begin{cases} Z_1 = \begin{bmatrix} z_1 \\ z_2 \end{bmatrix} = X_1 - R \\ Z_2 = \begin{bmatrix} z_3 \\ z_4 \end{bmatrix} = X_2 + \varphi(R) \end{cases} \quad (31)$$

Regarding  $Z_2$  as the control variable and according to Artstein's theorem [25], let find a globally stabilizing control law for the dynamics of  $X_1$  in Eq. (29). Let  $Z_2^{des} = -[\vartheta(Z_1 + R) - \vartheta(R)] = -\Delta\vartheta$  be a variable control law along with the control Lyapunov function  $W(Z_1) = \frac{1}{2}Z_1^T Z_1 = \frac{1}{2}z_1^2 + \frac{1}{2}z_2^2$ .

Taking the time derivative of  $W$  yields:

$$\dot{W}(Z_1) = (\varphi_1(z_1 + r_1) + z_3 - \varphi_1(r_1) - \dot{r}_1)z_1 + (\varphi_2(z_2 + r_2) + z_4 - \varphi_2(r_2) - \dot{r}_2)z_2 \quad (32)$$

for  $Z_2 = Z_2^{des}$ , it can be written as

$$\dot{W}/Z_2 = Z_2^{des} = (\Delta\varphi_1 - \Delta\vartheta_1 - \dot{r}_1)z_1 + (\Delta\varphi_2 - \Delta\vartheta_2 - \dot{r}_2)z_2 \quad (33)$$

in which  $\dot{W}$  is negative definite if A1 and A2 hold.

By introducing the residual  $\tilde{Z}_2 = Z_2 - Z_2^{des}$ , the system (29) can be rewritten in terms of  $Z_1$  and  $\tilde{Z}_2$ :

$$\begin{cases} \dot{Z}_1 = \Delta\varphi + Z_2 - \dot{R} \\ \dot{\tilde{Z}}_2 = V + \varphi'(R)\dot{R} - \frac{dZ_2^{des}}{dt} \end{cases} \quad (34)$$

so:

$$\begin{cases} \dot{Z}_1 = \Delta\varphi + Z_2^{des} + \tilde{Z}_2 - \dot{R} \\ \dot{\tilde{Z}}_2 = V + \varphi'(R)\dot{R} + \vartheta'_{Z_1}(Z_1 + R)\dot{Z}_1 + \vartheta'_R(Z_1 + R)\dot{R} - \vartheta'(R)\dot{R} \end{cases} \quad (35)$$

where  $\vartheta'_{Z_1}(Z_1 + R) = \frac{\partial\vartheta(Z_1+R)}{\partial Z_1}$  and  $\vartheta'_R(Z_1 + R) = \frac{\partial\vartheta(Z_1+R)}{\partial R}$  are two Jacobian matrix of  $\vartheta$ . Then:

$$\begin{cases} \dot{Z}_1 = \Delta\varphi - \Delta\vartheta + \tilde{Z}_2 - \dot{R} \\ \dot{\tilde{Z}}_2 = V + \vartheta'_{Z_1}(Z_1 + R)(\Delta\varphi - \Delta\vartheta + \tilde{Z}_2 - \dot{R}) + (\vartheta'_R(Z_1 + R) + \varphi'(R) - \vartheta'(R))\dot{R} \end{cases} \quad (36)$$

Let the control Lyapunov function  $\mathcal{W}(Z_1, \tilde{Z}_2) = F(Z_1) + \frac{1}{2}Z_2^T Z_2$  for the system (36), where  $F$  is any valid control Lyapunov function for the  $Z_1$ -subsystem. Then

$$\dot{\mathcal{W}}(Z_1, \tilde{Z}_2) = F'(Z_1)\dot{Z}_1 + \tilde{Z}_2^T \dot{\tilde{Z}}_2 \quad (37)$$

where the  $F'(Z_1)$  is the derivative of the scalar  $F(Z_1)$  with respect to the vector  $Z_1$ ,  $[F'(Z_1)]^T \in \mathbb{R}^2$ .

Consequently

$$\begin{aligned} \dot{\mathcal{W}}(Z_1, \tilde{Z}_2) &= F'(Z_1)(\Delta\varphi - \Delta\vartheta + \tilde{Z}_2 - \dot{R}) \\ &\quad + \tilde{Z}_2^T \left( V + \vartheta'_{Z_1}(Z_1 + R)(\Delta\varphi - \Delta\vartheta + \tilde{Z}_2 - \dot{R}) \right. \\ &\quad \left. + (\vartheta'_R(Z_1 + R) + \varphi'(R) - \vartheta'(R))\dot{R} \right) \end{aligned} \quad (38)$$

Let  $U(Z_1) = -F'(Z_1)(\Delta\varphi - \Delta\vartheta - \dot{R})$ , so:

$$\begin{aligned} \dot{\mathcal{W}}(Z_1, \tilde{Z}_2) &= -U(Z_1) + F'(Z_1)\tilde{Z}_2 \\ &\quad + \tilde{Z}_2^T \left( V + \vartheta'_{Z_1}(Z_1 + R)(\Delta\varphi - \Delta\vartheta + \tilde{Z}_2 - \dot{R}) \right. \\ &\quad \left. + (\vartheta'_R(Z_1 + R) + \varphi'(R) - \vartheta'(R))\dot{R} \right) \end{aligned} \quad (39)$$

which can be written as

$$\begin{aligned} \dot{\mathcal{W}}(Z_1, \tilde{Z}_2) &= -U(Z_1) \\ &\quad + \tilde{Z}_2^T \left( V + [F'(Z_1)]^T + \vartheta'_{Z_1}(Z_1 + R)(\Delta\varphi - \Delta\vartheta + \tilde{Z}_2 - \dot{R}) \right. \\ &\quad \left. + (\vartheta'_R(Z_1 + R) + \varphi'(R) - \vartheta'(R))\dot{R} \right) \end{aligned} \quad (40)$$

To reduce the complexity of the second term,  $F$  is selected such that the  $Z_1$  terms inside the bracket cancel each other. This is achieved by choosing  $F(Z_1)$  such as  $[F'(Z_1)]^T = -\vartheta'_{Z_1}(Z_1 + R)(\Delta\varphi - \Delta\vartheta - \dot{R}) - (\vartheta'_R(Z_1 + R) + \varphi'(R) - \vartheta'(R))\dot{R}$  and  $F(0) = 0$ .

Inserting this into Eq. (40), we obtain

$$\dot{\mathcal{W}}(Z_1, \tilde{Z}_2) = -U(Z_1) + \tilde{Z}_2^T (V + \vartheta'_{Z_1}(Z_1 + R)\tilde{Z}_2) \quad (41)$$

Let the following control law:

$$V = -(kI_2 + \vartheta'_{Z_1}(Z_1 + R))(Z_2 - Z_2^{des}) = -(kI_2 + \vartheta'_{Z_1}(Z_1 + R))\tilde{Z}_2 \quad (42)$$

where  $k \in \mathbb{R}^+$ . Then, Eq. (41) becomes

$$\dot{\mathcal{W}}(Z_1, \tilde{Z}_2) = -U(Z_1) - k\tilde{Z}_2^T \tilde{Z}_2 \quad (43)$$

Finally, if A3 holds, then  $U(Z_1) > 0$  and  $\dot{\mathcal{W}}$  is negative definite.  $\square$

#### 4.2. Backstepping liquid level controller design

The proposed Backstepping control law (30) can be applied to the state coupled four-tank system. So to apply this approach for the control of  $h_1$  and  $h_2$ , we write the process model (8) in a matrix form as follows:

$$\begin{cases} \dot{H}_1 = A \begin{bmatrix} \sqrt{h_1} \\ \sqrt{h_2} \end{bmatrix} + B \begin{bmatrix} \sqrt{h_3} \\ \sqrt{h_4} \end{bmatrix} \\ \dot{H}_2 = C \begin{bmatrix} \sqrt{h_3} \\ \sqrt{h_4} \end{bmatrix} + DU \\ Y = H_1 \end{cases} \quad (44)$$

where  $H_1 = \begin{bmatrix} h_1 \\ h_2 \end{bmatrix}$ ,  $H_2 = \begin{bmatrix} h_3 \\ h_4 \end{bmatrix}$ ,  $A = \begin{bmatrix} -c_1 & 0 \\ 0 & -c_4 \end{bmatrix}$ ,  $B = \begin{bmatrix} c_2 & c_3 \\ c_5 & c_6 \end{bmatrix}$ ,  $C = \begin{bmatrix} -c_7 & 0 \\ 0 & -c_9 \end{bmatrix}$ ,  
 $D = \begin{bmatrix} c_8 & 0 \\ 0 & c_{10} \end{bmatrix}$  and  $U = \begin{bmatrix} u_1 \\ u_2 \end{bmatrix}$ .

By choosing  $X_1 = H_1$ ,  $X_2 = B \begin{bmatrix} \sqrt{h_3} \\ \sqrt{h_4} \end{bmatrix}$  and  $\varphi(X_1) = A \begin{bmatrix} \sqrt{h_1} \\ \sqrt{h_2} \end{bmatrix}$ , we can write Eq. (44) in the form (29) as follows:

$$\begin{cases} \dot{X}_1 = \varphi(X_1) + X_2 \\ \dot{X}_2 = \frac{1}{2} B \begin{bmatrix} \frac{1}{\sqrt{h_3}} & 0 \\ 0 & \frac{1}{\sqrt{h_4}} \end{bmatrix} \left( C \begin{bmatrix} \sqrt{h_3} \\ \sqrt{h_4} \end{bmatrix} + DU \right) = V \end{cases} \quad (45)$$

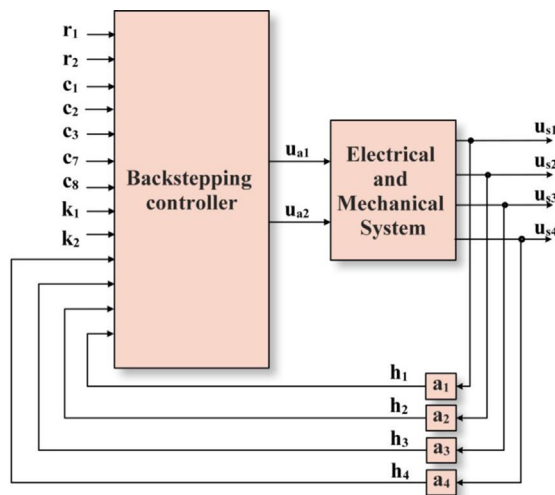


Fig. 4. Block diagram of the Backstepping approach.

Referring to the control law (30) and by choosing  $\vartheta(X_1) = k_1 X_1$ ,  $k_1 \in \mathfrak{R}$ , an auxiliary input for the system of Eq. (45) is defined and is given by

$$V = -(k + k_1)(\varphi(R) + X_2 + k_1(X_1 - R)) \quad (46)$$

with  $\varphi(R) = A \begin{bmatrix} \sqrt{r_1} \\ \sqrt{r_2} \end{bmatrix}$  which is globally Lipschitz ( $r_i > 1$ ,  $i = 1, 2$ ) and  $k > 0$ . A structure of Backstepping control law with state feedback can be suggested for the state coupled four-tank system. It is given by extracting  $U$  from the expression of  $V$  in Eq. (45) which can be written as:

$$V = \frac{1}{2} \begin{bmatrix} \frac{c_2}{\sqrt{h_3}} & \frac{c_3}{\sqrt{h_4}} \\ \frac{c_5}{\sqrt{h_3}} & \frac{c_6}{\sqrt{h_4}} \end{bmatrix} \left( \begin{bmatrix} -c_7\sqrt{h_3} \\ -c_9\sqrt{h_4} \end{bmatrix} + DU \right) \quad (47)$$

Finally, we obtain

$$U = \begin{bmatrix} u_1 \\ u_2 \end{bmatrix} = \begin{bmatrix} \frac{1}{c_8} & 0 \\ 0 & \frac{1}{c_{10}} \end{bmatrix} \left( \frac{1}{\alpha} \begin{bmatrix} c_6\sqrt{h_3} & -c_3\sqrt{h_3} \\ -c_5\sqrt{h_4} & c_2\sqrt{h_4} \end{bmatrix} V + \begin{bmatrix} c_7\sqrt{h_3} \\ c_9\sqrt{h_4} \end{bmatrix} \right) \quad (48)$$

with  $\alpha = \frac{1}{2}(c_2 c_6 - c_3 c_5)$ .

For implementing and tuning the designed controllers, we have used the same Simulink model of the nonlinear continuous-time system (8) which has been identified using real data as mentioned in Remark 1 at the laboratory “Study of Industrial Systems and Renewable Energies” at University of Monastir. Each controller has been implemented as a Simulink block and integrated in a Simulink control model similar to the simulation model used in the design stage. In the experimental setup, this Simulink control model communicates with the STM32 microcontroller of the real plant via the USB protocol to receive the measured level of the tanks and to send the calculated manipulated variables.

Concerning the possibilities of the controller design, the Backstepping control method has two control parameters ( $k$  and  $k_1$ ) and leads to an enhanced dynamic. However, the NGPC contains a predictive calculation of the actuating signal based on the system model. Thus, an improvement of the dynamic can be achieved. Due to the fact that the Predictive controller consists only of one control parameter ( $T_p$ ), this method is the easiest in control parameters tuning.

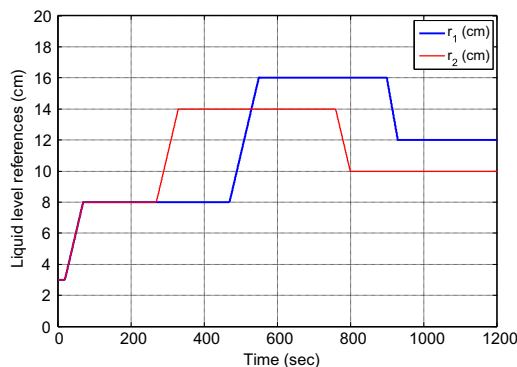


Fig. 5. Benchmark trajectories  $r_1$  and  $r_2$ .

Table 1

Numerical values for physical parameters of the system.

Physical quantity	Symbol	Numerical value
Tank 1 diameter	$D_{T1}$	$15\sqrt{2}$ cm
Tank 2 diameter	$D_{T2}$	$15\sqrt{2}$ cm
Tank 3 diameter	$D_{T3}$	$15\sqrt{2}$ cm
Tank 4 diameter	$D_{T4}$	$15\sqrt{2}$ cm
Tank 31 orifice diameter	$d_{31}$	0.38 cm
Tank 42 orifice diameter	$d_{42}$	0.38 cm
Tank 32 orifice diameter	$d_{32}$	0.31 cm
Tank 41 orifice diameter	$d_{41}$	0.31 cm
Tank 1 orifice diameter	$d_1$	0.48 cm
Tank 2 orifice diameter	$d_2$	0.48 cm
Pumps constant	$K_p$	$7.687 \text{ cm}^3/\text{V}$
Gravitational constant	$g$	$981 \text{ cm}/\text{s}^2$

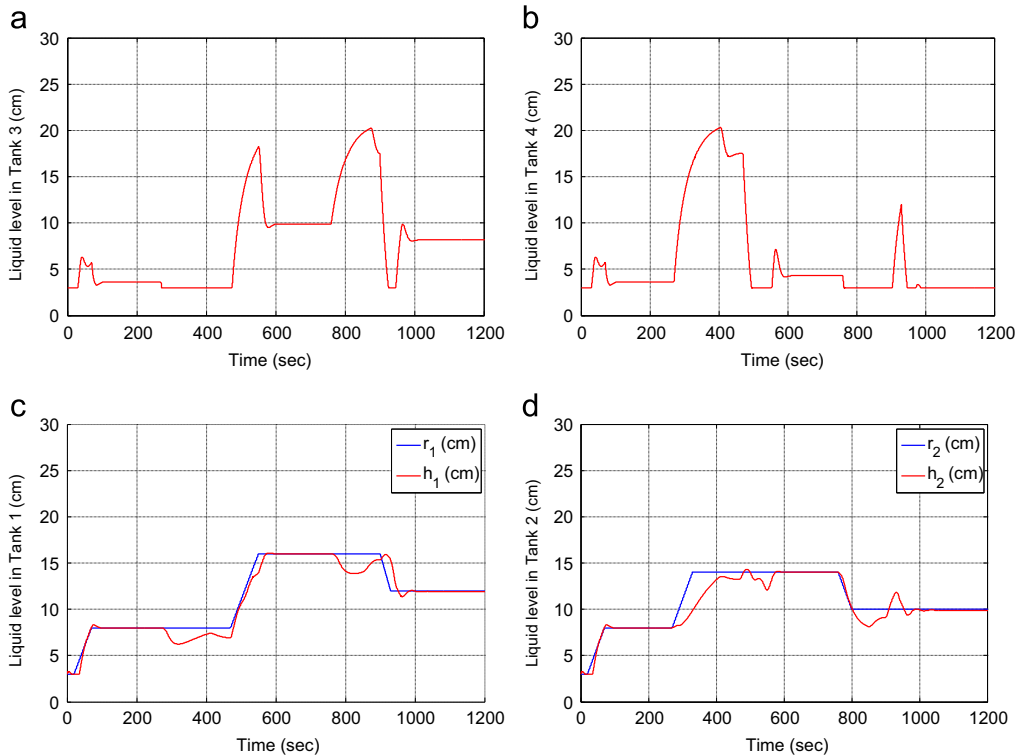


Fig. 6. Simulation results of Predictive control: liquid levels in the quadruple process.

Depending on the specific knowledge one might have, it might be easier for some users to design a Backstepping controller and for other users to design a Predictive controller. Comparing the Backstepping control method and the generalized Predictive controller in terms of their



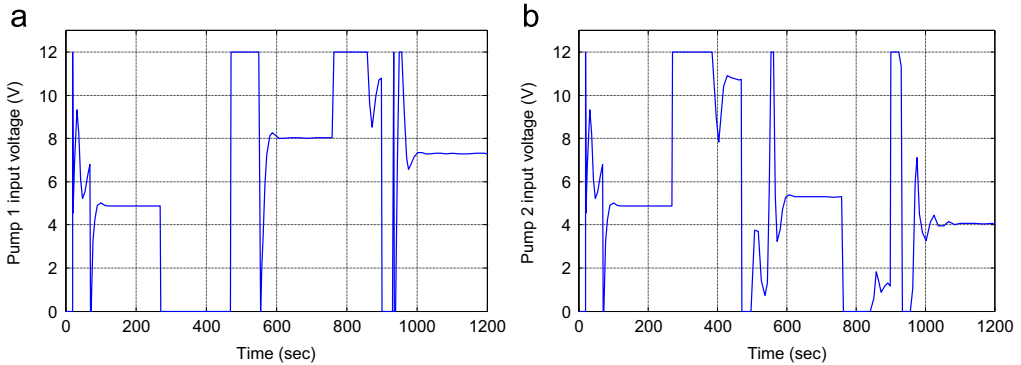


Fig. 7. Simulation results of Predictive control: Pump 1 and Pump 2 voltages.

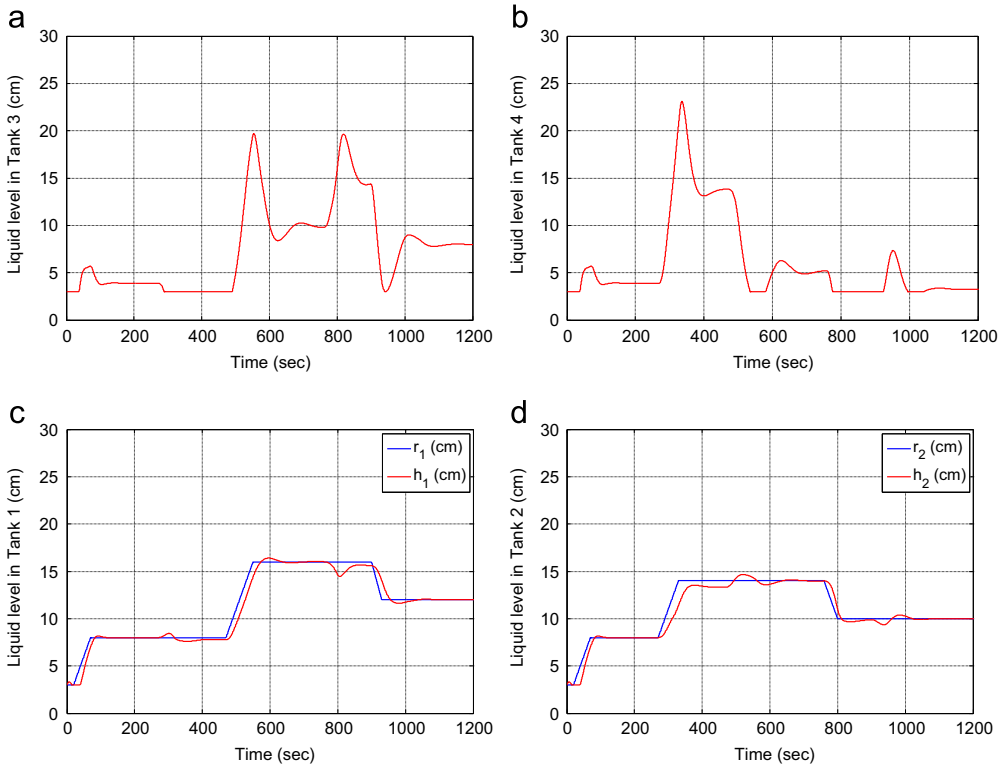


Fig. 8. Simulation results of Backstepping control: liquid levels in the quadruple process.

complexity of implementation, the Predictive is much higher than that of the Backstepping which is simpler in terms of the computational complexity and the mathematical development. This is can also be deduced from the difference between their block diagrams in Figs. 3 and 4. In the following sections, the different control techniques are presented together with the results of the control test in the real plant.

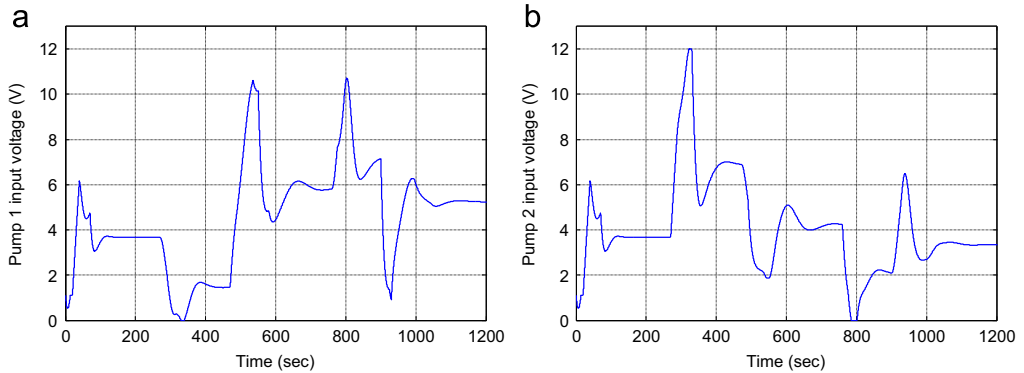


Fig. 9. Simulation results of Backstepping control: Pump 1 and Pump 2 voltages.

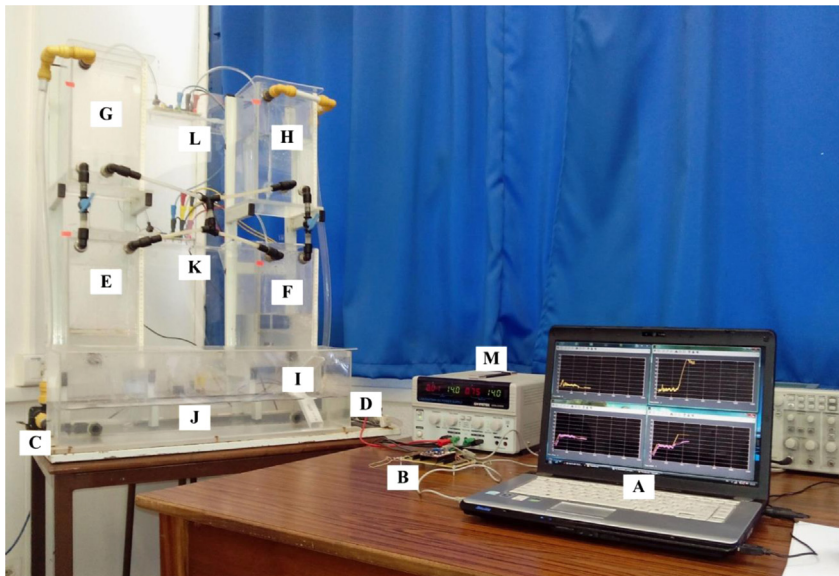


Fig. 10. Experimental setup: (A) control desk; (B) Fio std STM32F10 board; (C) Pump 1; (D) Pump 2; (E) Tank 1; (F) Tank 2; (G) Tank 3; (H) Tank 4; (I) Basin; (J) motor driver board; (K) liquid level sensors for Tank 1 and Tank 2; (L) liquid level sensors for Tank 3 and Tank 4; (M):  $\pm 14$  V supply voltage.

## 5. Simulation and experimental results

The closed-loop benchmark used by simulation and experimental validations, shown in Fig. 5, presents two different trapezoidal references  $r_1$  and  $r_2$  for respectively liquid levels  $h_1$  and  $h_2$ . The control test duration is 20 min. Each reference presents three level trajectories to allow a good evaluation of the proposed controllers. It is important to remark that the two references have been chosen in such a way that large changes in different equilibrium points are involved. These changes are applied at four times throughout the experiment: at 270 s, 470 s, 760 s and 900 s. This allows seeing the decoupling performance of system outputs.

For simulation and experimental validations, measurements are taken for each control method under the same conditions. The minimum and maximum levels of control signals are 0 and 12 V,

respectively, and the maximum liquid levels of tanks are 30cm. The sampling time is always equal to 0.01 s. The numerical values of the parameters for the studied four-tank liquid level system are given in Table 1.

**Remark 1.** Before deriving the main results, it is necessary that the model be as faithful as possible to the real system. Since the two proposed control designs are based on the intrinsic nonlinear system dynamics, they use the system parameters to provide the control signals. System parameters  $c_i$   $i = 1, \dots, 10$  are so firstly calculated from the physical parameters of the state coupled four-tank system according their expressions in Eq. (7). Then, for more accuracy in the system modeling, the real system (Fig. 10) and the model (8) are several controlled simultaneously in open loop and these parameters are tuned until best accuracy between the system and the model outputs.

### 5.1. Simulation results

The two nonlinear controllers are firstly implemented in the simulation setup. It is shown that they give good tracking performances with negligible tracking error, but with input signals having an important portion outside the range of the real actuators (9).

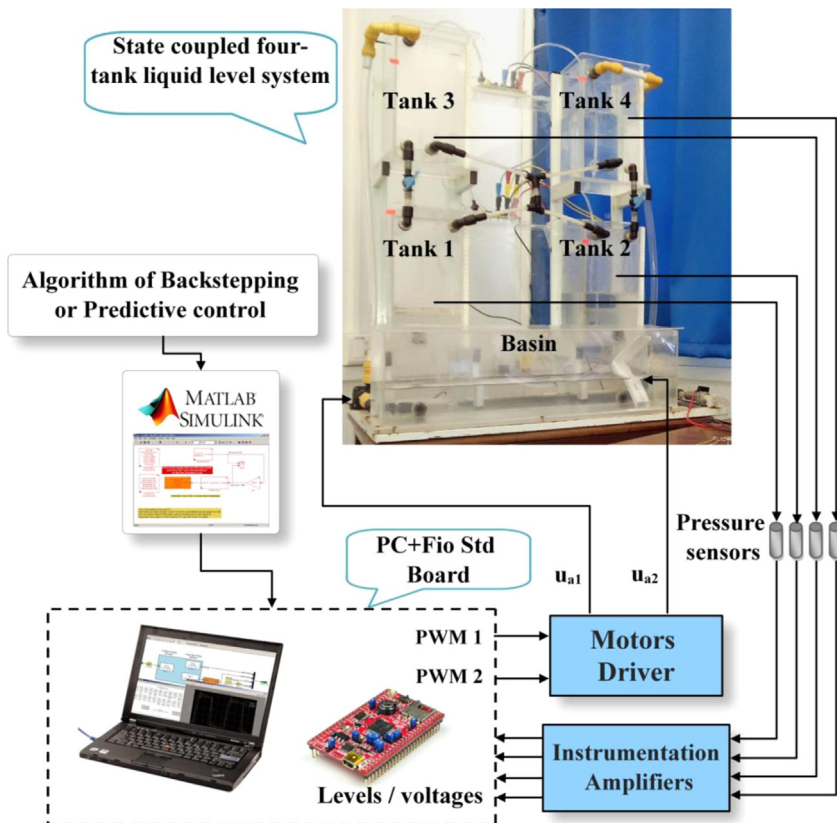


Fig. 11. Synoptic scheme of the setup.

Consequently, it is important to take into account the input saturation (9) in the choice of the parameters of each control approach in the simulation validation. In fact, parameters  $k$  and  $k_1$  for the Backstepping controller and  $T_p$  for the NGPC law are chosen in order to make the control input signals between the saturation limits by minimizing as much as possible the portion of the control signal which falls outside the range of the actuators.

The model-based Predictive and Backstepping control laws given in Eqs. (28) and (48) are implemented with respect to the input saturation on the same simulation apparatus which is performed by a MATLAB/Simulink model of the real process. The prediction horizon is chosen in order to satisfy a compromise between the stability of the closed loop and the computational time requirement. It is tuned by trial-and error until good performance with  $T_p = 11$  s. On the other hand, the control gains of the Backstepping controller are tuned by trial-and error until the best tracking performance with input control signals falling in the range of the actuators. Their values are finally given as:  $k = 0.03$  and  $k_1 = 0.088$ . The simulation results of the four liquid levels with tracking responses are illustrated in Figs. 6 and 8 and the pumps input voltages are illustrated in Figs. 7 and 9.

According to Figs. 6 and 8, it can be observed that the Backstepping controller gives better performances than the predictive one. With less aggressive control signals (Fig. 9), it gives a better tracking response with better disturbance rejection. Indeed, while the tracking performance of the predictive controller degrades under inputs saturation in the reference changes, the performance of the Backstepping controller remains virtually the same.

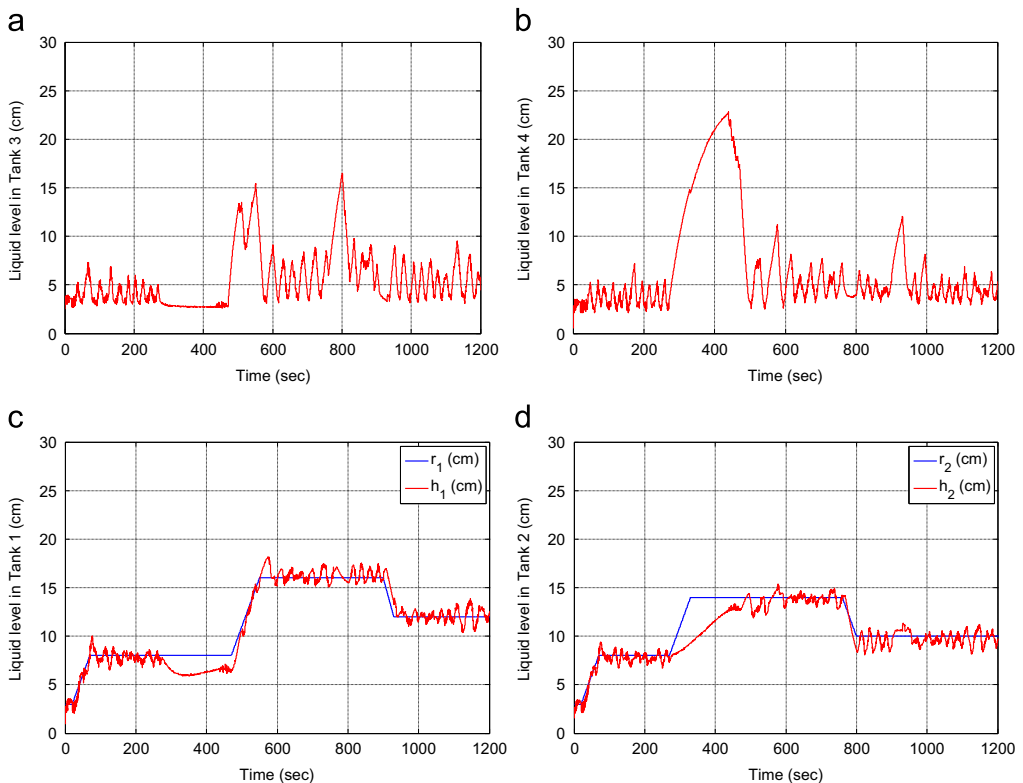


Fig. 12. Experimental results of Predictive control: liquid levels in the quadruple process.

**Remark 2.** Note that while deriving the simulation results, the choice of the parameters must be done in the order that liquid levels in Tanks 3 and 4 do not exceed 30 cm. If not, we will have problems in the experiments because all tanks are of 30 cm maximum height. This presents a further constraint in the tuning of control parameters.

## 5.2. Experimental results

The nonlinear model-based Predictive and Backstepping controllers are implemented on an experimental, four-tank, liquid level system, shown in Fig. 10, located in the laboratory “Study of Industrial Systems and Renewable Energies” at National Engineers School of Monastir, Tunisia.

The system consists of the four-tank module, electromechanical system with the data acquisition and control hardware/software. The two proposed control schemes have been implemented in the MATLAB/Simulink environment combined with the real time interface associated to the STM32 microcontroller data acquisition device. The synoptic scheme of the proposed controllers used in the experimental setup is presented in Fig. 11.

In the experimental setup, the conversion Voltage/Level of the four measured sensors voltages  $u_{s1}$ ,  $u_{s2}$ ,  $u_{s3}$  and  $u_{s4}$  is made by multiplying respectively by the coefficients  $a_1 = 9.4458 \text{ cm V}^{-1}$ ,  $a_2 = 8.7106 \text{ cm V}^{-1}$ ,  $a_3 = 8.5106 \text{ cm V}^{-1}$  and  $a_4 = 9.3458 \text{ cm V}^{-1}$ .

The state coupled four-tank system is required to track the two trajectories under the control of the original NGPC and the Backstepping techniques. The model-based Predictive control law given in Eq. (28) is firstly implemented in real time with respect to the synoptic scheme and the inputs saturation. The prediction horizon is chosen with respect to the simulation results. The experimental tracking results are illustrated in Fig. 12(c) and (d). The tracking errors are given in Fig. 13 and the pumps input voltages are illustrated in Fig. 14. We see that the liquid levels  $h_1$  and  $h_2$  trajectories track their references with negligible static error even the consideration of the inputs saturation in the controller.

Additionally, the model-based Backstepping control law given in Eq. (48) is implemented in real time on the same experimental apparatus. The same control gains  $k_1$  and  $k_2$  are used. The experimental tracking results are illustrated in Fig. 15(c) and (d). The tracking errors are given in Fig. 16 and the pumps input voltages are illustrated in Fig. 17. It can be also observed that the

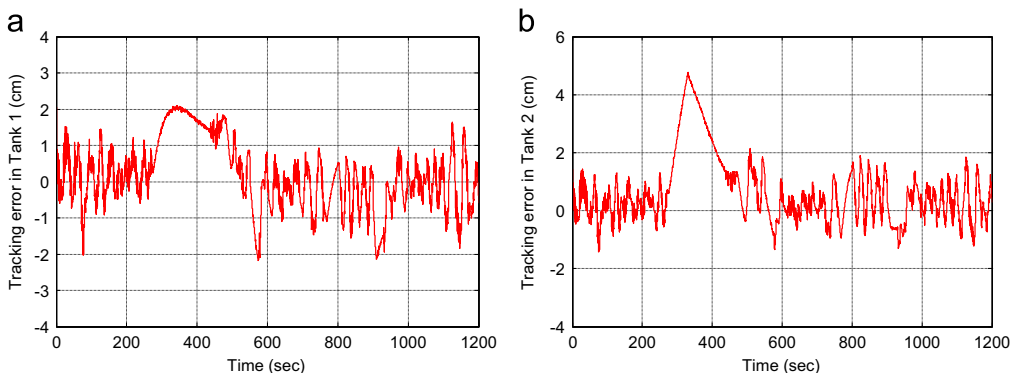


Fig. 13. Experimental results of Predictive control: tracking errors in Tank 1 and Tank 2.

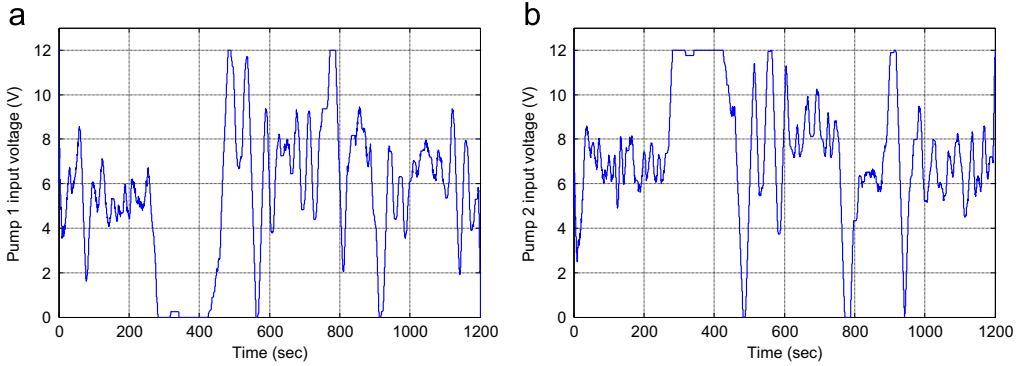


Fig. 14. Experimental results of Predictive control: Pump 1 and Pump 2 voltages.

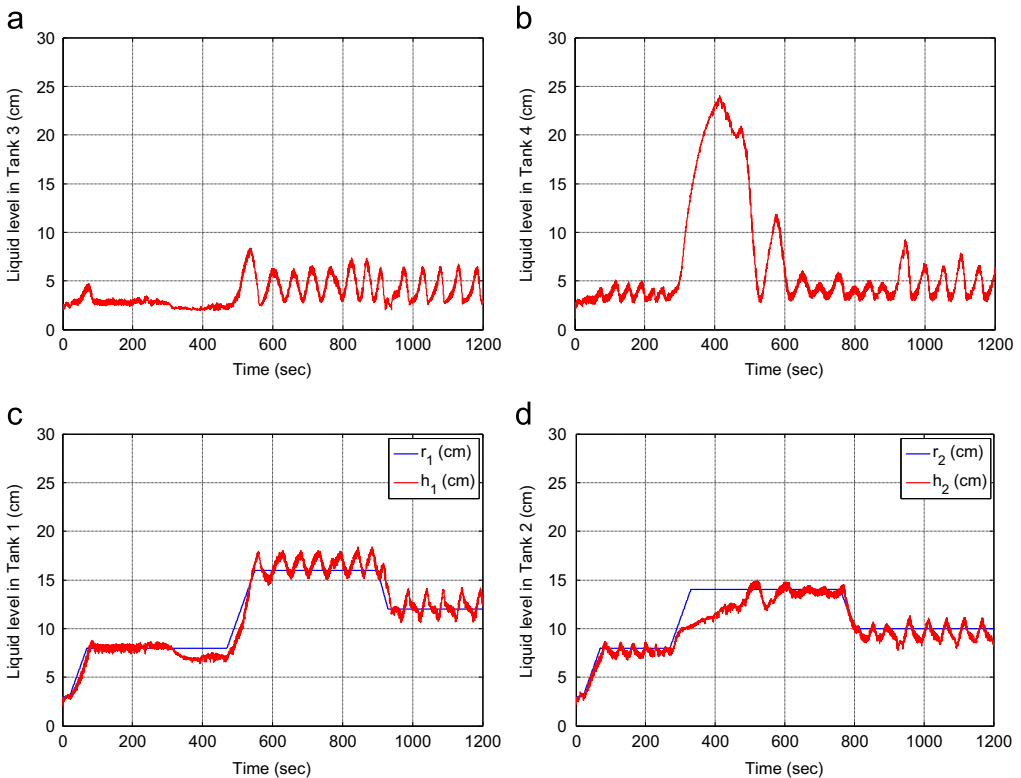


Fig. 15. Experimental results of Backstepping control: liquid levels in the quadruple process.

liquid levels  $h_1$  and  $h_2$  track their references without noticeable perturbations, even if the references  $r_1$  and  $r_2$  change their levels.

**Remark 3.** While conducting experiments on the model-based controllers, the Backstepping control gains  $k_1$  and  $k_2$  are tuned using the following steps (Same method for the predictive period  $T_p$ ):

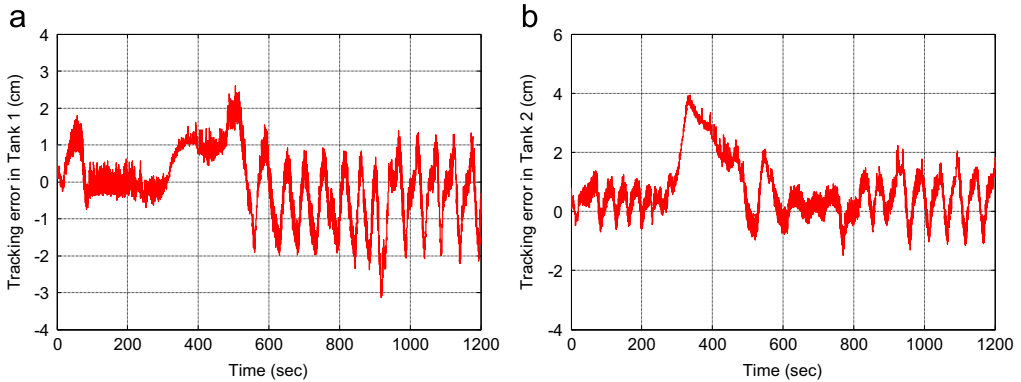


Fig. 16. Experimental results of Backstepping control: tracking errors in Tank 1 and Tank 2.

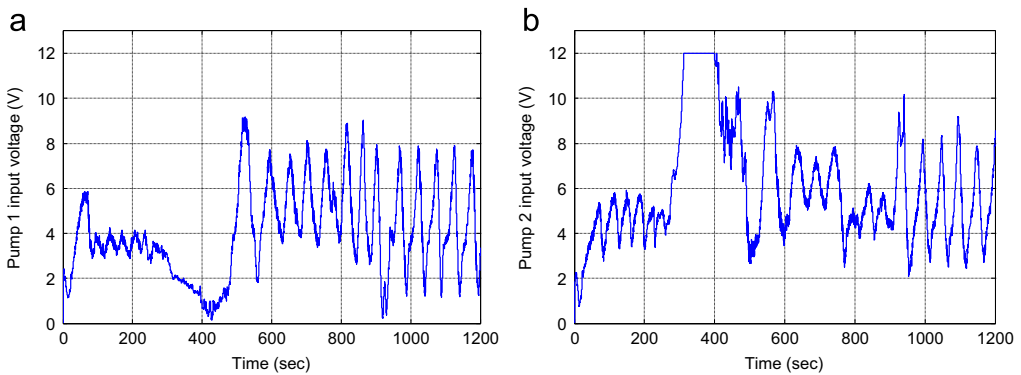


Fig. 17. Experimental results of Backstepping control: Pump 1 and Pump 2 voltages.

- (1) Use a desired trajectory that is not too demanding (e.g., slow time-varying step-like inputs).
- (2) Choose a set of initial control gains ( $k_1, k_2$ ).
- (3) Tune the control gains to obtain a good trajectory tracking response.
- (4) Replace the slow time-varying step-like inputs with trapezoidal-like inputs such that the desired trajectories are not very aggressive initially.
- (5) Iterate steps 3–4 on the new trajectories to obtain good performance, if necessary, taking into account the problem outlined in Remark 2.

**Remark 4.** While deriving the experimental results, the main difficulty met is that both pumps do not always run with inputs voltage  $u_i \leq 3V$ ,  $i = 1, 2$ . This causes that the response loses its benchmark during the experiment and then a failure of the control test. The experiment must so be repeated until an acceptable experimental result despite a little difference observed with the simulation one.

It can be observed that experimental results are close to the simulation ones. Nevertheless, due to measurement noise, none considered actuator dead zones (outlined in Remark 4) and imperfection parameters knowledge, some differences appear.



### 5.3. Comparison of the measurement results

This section discusses the different schemes of controllers in the aspects of experimental tracking performances. Several control tests have been designed to investigate the control performance of the proposed control schemes on the real liquid level system.

It can be seen that both the Backstepping and the NGPC controllers are able to deal with the uncertainties, achieve trajectory tracking, and compensate the steady state error in the presence of the input saturation, but they have side-effects like overshoot and aggressive control, especially for the NGPC approach.

Following the benchmark of the system, the two references  $r_1$  and  $r_2$  firstly change simultaneously from 3 cm to 8 cm at 20 s. It can be observed, for the two controllers, that the liquid levels  $h_1$  and  $h_2$  track their trajectories in a similar manner. At 270 s, the reference  $r_2$  changes to 14 cm. This change causes an enlargement of the tracking error of liquid level  $h_1$  in the case of NGPC law. However, the Backstepping controller exhibits better performance under this change and maintains a lower tracking error. At 470 s, the reference  $r_1$  changes to 16 cm. This change causes an enlargement of the tracking error of liquid level  $h_2$  in the case of the both control laws for an important time period. This is due to the maintaining constant of  $h_1$  by the controllers. Finally, at 760 s,  $r_2$  changes to 10 cm and at 900s  $r_1$  changes its level to 12 cm. These changes cause small perturbations for the tracking performance of the controlled liquid levels  $h_1$  and  $h_2$  for the two controllers.

With the NGPC approach, a global better response is achieved with a better precision performance (Fig. 13). However, the Backstepping controller introduces a more important tracking error throughout the experiment (Fig. 16). Additionally, the NGPC law tested can potentially deal with the satisfaction of hard inputs constraints and states of the plant under appropriate assumptions. However, the system's dynamic seems more robust against input saturation under the Backstepping law. Indeed, it can be shown that it follows from the experimental results that the good tracking performance of the Predictive controller is obtained at the price of higher control effort. This means that the Backstepping's input signal is more efficient than the Predictive's one.

The main experimental disadvantage of the used Backstepping approach is the noticeable fluctuations of the responses  $h_1$  and  $h_2$  around their references 16–14 cm and 12 cm. Although we performed several experimental tests of this controller using many parameters configurations, we failed to cancel these fluctuations in these levels. This disadvantage can be avoided by introducing other further Backstepping methods in [29–32].

The robustness concerning parameter uncertainties are analyzed by varying the system parameters of the mechanical systems  $c_1$ ,  $c_2$ ,  $c_3$ ,  $c_7$  and  $c_8$ , whereas the two controllers are tuned for the nominal

Table 2  
Comparison of the proposed liquid level control approaches.

Comparison criteria	Liquid level control method	
	Predictive	Backstepping
Relative stability	Good	Excellent
Robustness concern uncertain parameters	Medium	Good
Robustness concern input saturation	Good	Excellent
Precision performance	Excellent	Good
Possibilities of controller design	Medium	Medium
Complexity of parameters tuning	Low	High
Complexity of implementation	High	Low

system. An experimental validation of both proposed controllers has been performed for each parameter variation. It can be seen that both the considered control methods yield stable control loops for the uncertain system, but the Backstepping-based control is more robust than NGPC.

Note that, all the controllers considered have demonstrated good properties in the closed-loop experiments carried out, exhibiting stable and feasible trajectories in spite of the input saturation and mismatches between the prediction model and the plant.

Some results obtained based on the theoretical and practical analyses are summarized in Table 2. The measurements results confirmed that the two approaches provide quite good performance for both simulations and experiments. They have high stability and robustness properties. The proposed Backstepping control is stable and robust with respect to the parameter uncertainties presented than the Predictive control.

**Remark 5.** Compared to the existing works already reported in the literature [2–6,16,26], the proposed robust controllers give also acceptable results without linearization of the system model or adjustment of the structure of the controller. Indeed, the desired performances are well achieved in the presence of the control input saturation as well as the large changes in different equilibrium points in the used benchmark.

## 6. Conclusion

This paper used Predictive and Backstepping techniques to develop nonlinear controllers for precise liquid level tracking in a state-coupled four-tank system. The nonlinear tracking control is achieved by an explicit NGPC algorithm, which eliminates the computationally intensive online optimization in traditional MPC. Additionally, a second controller based on the Backstepping strategy is designed that ensures asymptotic global stability for the system.

Experimental results were presented to illustrate the improved performance of the proposed nonlinear controllers as well as a detailed comparison of the two different control methods were presented in terms of their dynamic behavior and their stability as well as their robustness properties.

For comparability, the measurements were taken for each control method under the same operating conditions. In both cases, the closed-loop process is stabilized and it can be concluded that the Backstepping control method is easier to design and to implement but the tracking error for the Predictive controller is better.

Finally, the user has to decide depending on the required control performance and the available control hardware, which, of the two control methods presented in this paper, is the most convenient one.

## Acknowledgment

This work was supported by the University of Monastir. This support is very gratefully acknowledged by the authors. Moreover, H. Gouta expresses appreciation for the fellowship from the Research Unit of Industrial Systems Study and Renewable Energy.

## References

- [1] R.N. Bateson, *Introduction to Control System Technology*, 6th ed., Prentice-Hall, Upper Saddle River, NJ, 1999.
- [2] K.H. Johansson, The quadruple-tank process: a multivariable laboratory process with an adjustable zero, *IEEE Trans. Control. Syst. Technol.* 8 (2000) 456–465.

- [3] E.P. Gatzke, E.S. Meadows, C. Wang, F.J. Doyle III, Model based control of a four-tank system, *Comput. Chem. Eng.* 24 (2000) 1503–1509.
- [4] L. Dai, K.J. Åström, Dynamic Matrix Control of a Quadruple Tank Process, IFAC World Congress, 1999.
- [5] R. Vadigepalli, E.P. Gatzke, F.J. Doyle III, Robust Control of a Multivariable Experimental 4-Tank System, University of Delaware, Newark, DE 19716, 2000.
- [6] M. Mercangöz, F.J. Doyle III, Distributed model predictive control of an experimental four-tank system, *J. Process. Control* 17 (2007) 297–308.
- [7] Y. Yang, D. Yue, Y. Xue, Decentralized adaptive neural output feedback control of a class of large-scale time-delay systems with input saturation, *J. Frankl. Inst.* 352 (5) (2015) 2129–2151.
- [8] C.Y. Wen, J. Zhou, Z.T. Liu, H.Y. Su, Robust adaptive control of uncertain nonlinear systems in the presence of input saturation and external disturbance, *IEEE Trans. Autom. Control.* 56 (2011) 1672–1678.
- [9] M. Chen, S.S. Ge, B.B. Ren, Adaptive tracking control of uncertain MIMO nonlinear systems with input constraints, *Automatica* 47 (2011) 452–455.
- [10] E. Camacho, C. Bordons, *Model Predictive Control*, Springer, 1998.
- [11] M. Krstić, A. Smyshlyaev., *Boundary Control of PDE's: A Course on Backstepping Designs*, SIAM, Society for Industrial and Applied Mathematics, 2008.
- [12] D.Q. Mayne, J.B. Rawlings, C.V. Rao, P.O.M. Scokaert, Constrained model predictive control: stability and optimality, *Automatica* 36 (2000) 789–814.
- [13] S. Hadj Saïd, F. M'Sahli, M.F. Mimouni, M. Farza, Adaptive high gain observer based output feedback predictive controller for induction motors, *Comput. Electr. Eng.* 39 (2013) 151–163.
- [14] W. Chen, D. Ballance, P. Gawthrop, Optimal control of nonlinear systems: a predictive control approach, *Automatica* 39 (2003) 633–641.
- [15] W. Chen, Predictive control of general nonlinear systems using approximation, *IEE Proc. Cont. Theory Appl.* 151 (2004) 137–143.
- [16] Y. Alipouri, J. Poshtan, Optimal controller design using discrete linear model for a four tank benchmark process, *ISA Trans.* 52 (5) (2013) 644–651.
- [17] H. Wang, X. Liu, K. Liu, Adaptive neural data-based compensation control of non-linear systems with dynamic uncertainties and input saturation, *IET Control. Theory Appl.* 9 (7) (2015) 1058–1065.
- [18] I. Kanellakopoulos, P.V. Kokotović, A. Morse, A toolkit for nonlinear feedback design, *Syst. Control Lett.* 18 (1992) 83–92.
- [19] A. Ouali, M. Fruchard, E. Courtial, Y. Tourré, A comparative study for the boundary control of a reaction-diffusion process: MPC vs backstepping, in: IFAC NMPC'12, Noordwijkerhout, Netherlands, 2012, pp. 200–206.
- [20] S. Thomsen, N. Hoffmann, F. Wilhelm, PI control, PI-based state space control, and model-based predictive control for drive systems with elastically coupled loads—a comparative study, *IEEE Trans. Ind. Electron.* 58 (8) (2011) 3647–3657.
- [21] K. Ogata, *System Dynamics*, 1st ed., Prentice-Hall, Englewood Cliffs, NJ, 1978.
- [22] M. Krstić, D. Fontaine, P.V. Kokotovic, J.D. Paduano, Useful nonlinearities and global stabilization of bifurcations in a model of jet engine surge and stall, *IEEE Trans. Autom. Control* 43 (1998) 1739–1745.
- [23] H. Gouta, S. Hadj Saïd, N. Barhoumi, F. M'Sahli, observer-based backstepping controller for a state-coupled two-tank system, *IETE J. Res.* 61 (2015) 258–267.
- [24] N. Barhoumi, M. F. M'sahli, Djemaï, K. Busawon, Observer design for some classes of uniformly observable nonlinear hybrid systems, *Nonlinear Anal.: Hybrid Syst.* 6 (2012) 917–929.
- [25] Z. Artstein, Stabilization with relaxed controls, *Nonlinear Anal. Theory, Methods Appl.* 7 (1983) 1163–1173.
- [26] V. Kirubakaran, T.K. Radhakrishnan, N. Sivakumaran, Distributed multiparametric model predictive control design for a quadruple tank process, *Measurement* 47 (2014) 841–854.
- [27] H. Pan, H. Wong, V. Kapila, M.S. de Queiroz, Experimental validation of a nonlinear backstepping liquid level controller for a state coupled two tank system, *Control. Eng. Pract.* 13 (2005) 27–40.
- [28] J. Rawlings, D. Mayne, *Model Predictive Control Theory and Design*, Nob Hill Pub, 2009.
- [29] J. Wu, W. Chen, F. Yang, J. Li, Q. Zhu, Global adaptive neural control for strict-feedback time-delay systems with predefined output accuracy, *Inform. Sci.* 301 (2015) 27–43.
- [30] J. Wu, W. Chen, J. Li, Fuzzy-approximation-based global adaptive control for uncertain strict-feedback systems with a priori known tracking accuracy, *Fuzzy Sets Syst.* (2014) <http://dx.doi.org/10.1016/j.fss.2014.10.009>.
- [31] J. Wu, J. Li, W. Chen, Semi-globally/globally stable adaptive NN backstepping control for uncertain MIMO systems with tracking accuracy known a priori", *J. Frankl. Inst.* 351 (12) (2014) 5274–5309.
- [32] J. Wu, W. Chen, D. Zhao, J. Li, Globally stable direct adaptive backstepping NN control for uncertain nonlinear strict-feedback systems, *Neurocomputing* 122 (12) (2013) 134–147.

- [33] Hassan K Khalil, Nonlinear Systems, 3rd ed., Prentice-Hall, Upper Saddle River, NJ, 2002.
- [34] C. Liu, W.-H. Chen, J. Andrews, Tracking control of small-scale helicopters using explicit nonlinear MPC augmented with disturbance observers, *Control. Eng. Pract.* 20 (2012) 258–268.
- [35] N.O. Perez-Arancibia, T.-C. Tsao, J.S. Gibson, Saturation-induced instability and its avoidance in adaptive control of hard disk drives, *IEEE Trans. Control. Syst. Technol.* vol. 18 (2010) 368–382.
- [36] H. Wang, B. Chen, X. Liu, K. Liu, C. Lin, Adaptive neural tracking control for stochastic nonlinear strict-feedback systems with unknown input saturation, *Inform. Sci.* 269 (2014) 300–315.
- [37] Y.-Y. Cao, Z. Lin, Min-max MPC algorithm for LPV systems subject to input saturation, *IEE Proc. Control. Theory Appl.* 152 (3) (2005) 266–272.
- [38] H. Huang, D. Li, Z. Lin, Y. Xi, An improved robust model predictive control design in the presence of actuator saturation, *Automatica* 47 (4) (2011) 861–864.
- [39] T. Shi, H. Su, J. Chu, An improved model predictive control for uncertain systems with input saturation, *J. Frankl. Inst.* 350 (9) (2013) 2757–2768.
- [40] T. Shi, H. Su, J. Chu, Sampled-data MPC for LPV systems with input saturation”, *IET Control. Theory Appl.* 8 (17) (2014) 1781–1788.



**Houssemeddine Gouta** was born in Sousse, Tunisia, in July 1985. He received his Engineering diploma and Master degree, respectively, in Electrical Engineering in 2009 and in Automatic and Signal Processing in 2010 from the National School of Engineer of Tunis, Tunisia (L'Ecole Nationale d'Ingénieurs de Tunis E.N.I.T). He is currently a Ph.D. candidate at Electrical Engineering in National Engineering School of Monastir. His research interests are focused on nonlinear control, theoretical aspects of nonlinear observer design and control of liquid level systems.



**Salim Hajd Said** received his M.S. degree in Automatic and Signal Processing and his Ph.D. in Electrical Engineering from National Engineering School of Tunis, in 2004 and 2009, respectively. He is currently an assistant professor of Automatic at Preparatory Institute for Engineering Studies of Monastir, Tunisia. His research interests include state observation, predictive and adaptive control of linear and nonlinear systems.



**Faouzi M'Sahli** received his B.S. and M.S. degrees from ENSET, Tunis, Tunisia in 1987 and 1989, respectively. In 1995, he obtained his Ph.D. degree in Electrical Engineering from ENIT, Tunisia. He is currently a professor of Electrical Engineering at National School of Engineers, Monastir, Tunisia. His research interests include modeling, identification, predictive and adaptive control of linear and nonlinear systems. He has published over 80 technical papers and is a co-author of a book 'Identification et commande numérique des procédés industriels', Technip editions, Paris.